Direct numerical simulation of helical magnetohydrodynamic turbulence with TARANG code

1st Rodion Stepanov
Institute of Continuous Media Mechanics
Perm Federal Research Center
Ural Branch Russian Academy of Sciences
Perm, Russia
rodion@icmm.ru

2nd Andrei Teimurazov
Institute of Continuous Media Mechanics
Perm Federal Research Center
Ural Branch Russian Academy of Sciences
Perm, Russia

3rd Valerij Titov
Institute of Continuous Media Mechanics
Perm Federal Research Center
Ural Branch Russian Academy of Sciences
Perm, Russia

4th Mahendra K. Verma
Department of Physics
Indian Institute of Technology
Kanpur, India

5th Satyajit Barman
Department of Physics
Indian Institute of Technology
Kanpur, India

6th Abhishek Kumar
Department of Physics
Indian Institute of Technology
Kanpur, India

7th Franck Plunian
Université Grenoble Alpes
Institut des Sciences de la Terre
Grenoble, France

***Abstract*—Magnetohydrodynamic (MHD) turbulence is an intrinsic part of astrophysical phenomena, which plays a crucial role is the generation of cosmic magnetic fields. The two-scale dynamo concept suggests that the small scale interactions are demanded to drive the large scale magnetic fields of planets, stars and galaxies. Since experimental study of MHD turbulence is almost impossible the numerical simulation is only a way to verify theoretical ideas and phenomenology. The purpose of this work is to demonstrate the possibilities of direct numerical simulation of MHD turbulence using the TARANG code (open source software). We focus on mathematical formulation and the built-in postprocessing functions for analysis of spectral distributions and transfers of energies and helicities in the forced 3D homogeneous isotropic MHD turbulence.**

***Index Terms*—direct numerical simulations, MHD turbulence, pseudospectral code, energy and helicity spectral transfers**

I. Introduction

Magnetohydrodynamic (MHD) turbulence is an intrinsic part of astrophysical phenomena, which plays a crucial role is the generation of cosmic magnetic fields. The two-scale dynamo concept suggests that the small scale interactions are demanded to drive the large scale magnetic fields of planets, stars and galaxies [1], [2]. Current phenomenology obtained for the mean hydrodynamic flows has a satisfactory agreement with experiment and allows to solve various engineering problems. However, the permanent complication of technology and the optimization of parameters require more precise solutions. The intensive development of computer technology in recent decades has brought to the forefront computer modeling as the main research tool. For MHD turbulence this is especially important, since conducting a laboratory experiment is almost impossible [3]. Description of turbulent flows of a continuous medium remains one of the most acute modern problems of the mechanics of gas, liquid, and plasma. The problems to be solved concern both the fundamental questions of geo- and astrophysics, and the applied problems arising in the development of new technologies.

Software packages of applied problems have become widely spread, allowing to take into account the turbulent nature of the motion. Typically the task is not solved in all its details, but a certain model of turbulence is used. In problems with complex geometry or in case of several active fields (convection, MHD, active chemistry) verification is required. This might be done experimentally, which is usually very expensive or impossible at all, or resort to complete direct numerical modeling. In the latter case, the success of a study will depend on the computational efficiency of the method and the flexibility in the formulation of the numerical setup.

At present, methods that are applicable for direct numerical simulation are constantly developing. Most codes are based on numerical algorithms using finite elements, finite volumes, finite differences or spectral representation. A comparative analysis of these methods involves a lot of research, which are not discussed here. The purpose of this work is to demonstrate the possibilities of direct numerical simulation of turbulence

0-7695-6356-2/17/$31.00 ©2017 IEEE
DOI 10.1109/ISPRAS.2017.00022

using the TARANG code [4]. Its advantages include: top performance and scalability characteristics, multi-physics, open source software is freely distributed, constantly updated by an actively working group of researchers, has a transparent configuration for rapid development and use. In this paper, we focus on the built-in postprocessing functions for analysis of spectral distributions and spectral energy and helicity transfers in homogeneous and isotropic MHD turbulence forced in a cubic region with periodic boundaries. As far as we know, such self-consistent mathematical description and numerical realization is suggested for the first time.

II. Mathematical formalism

A. MHD equations

The MHD equations that describe the dynamics of an incompressible and electrically conducting fluid are given by

$$\frac{\partial \mathbf{u}}{\partial t} = -\nabla P + \mathbf{u}\times\boldsymbol{\omega} + \mathbf{J}\times\mathbf{B} + \nu\nabla^2\mathbf{u} + \mathbf{F}, \quad (1)$$

$$\frac{\partial \mathbf{B}}{\partial t} = \nabla\times(\mathbf{u}\times\mathbf{B}) + \eta\nabla^2\mathbf{B}, \quad (2)$$

$$\nabla\cdot\mathbf{u} = 0, \quad (3)$$

$$\nabla\cdot\mathbf{B} = 0, \quad (4)$$

where $\mathbf{u}$ is the velocity, P is the normalized pressure (p/ρ_0), $\mathbf{B}$ is the normalized magnetic field ($\mathbf{b}/\sqrt{\mu\rho_0}$), $\mathbf{J} = \nabla\times\mathbf{B}$ is the current density, $\boldsymbol{\omega} = \nabla\times\mathbf{u}$ is the vorticity and $\mathbf{F}$ is the external force. Here ρ_0, ν, and $\eta = (\sigma\mu)^{-1}$ denote the fluid mean density, the kinetic viscosity, and the magnetic diffusivity, σ and μ being the electrical conductivity and the magnetic permeability.

We decompose the velocity and magnetic fields in the Fourier space as

$$\mathbf{u}(\mathbf{r},t) = \sum_{\mathbf{k}} \mathbf{u}(\mathbf{k},t)\exp(i\mathbf{k}\cdot\mathbf{r}), \quad (5)$$

$$\mathbf{B}(\mathbf{r},t) = \sum_{\mathbf{k}} \mathbf{B}(\mathbf{k},t)\exp(i\mathbf{k}\cdot\mathbf{r}), \quad (6)$$

where the wavevector $\mathbf{k} = (k_x, k_y, k_z)$ satisfies

$$k_x = \frac{2\pi l}{L_x};\ k_y = \frac{2\pi m}{L_y};\ k_z = \frac{2\pi n}{L_z}, \quad (7)$$

$L_x \times L_y \times L_z$ denoting the box size and l, m, n being integers. For convenience the Fourier coefficients $\mathbf{u}(\mathbf{k},t)$ and $\mathbf{B}(\mathbf{k},t)$ will be denoted $\mathbf{u}(\mathbf{k})$ and $\mathbf{B}(\mathbf{k})$, with implicit time dependency. This convention is followed throughout the paper.

In Fourier space (1) to (4) take the following form

$$\dot{\mathbf{u}}(\mathbf{k}) = \sum_{\triangle\mathbf{kpq}} \mathbf{u}^*(\mathbf{p})\times\boldsymbol{\omega}^*(\mathbf{q}) + \mathbf{J}^*(\mathbf{p})\times\mathbf{B}^*(\mathbf{q}) - iP(\mathbf{k})\mathbf{k} - \nu|\mathbf{k}|^2\mathbf{u}(\mathbf{k}) + \mathbf{F}(\mathbf{k}), \quad (8)$$

$$\dot{\mathbf{B}}(\mathbf{k}) = i\mathbf{k}\times\sum_{\triangle\mathbf{kpq}} \mathbf{u}^*(\mathbf{p})\times\mathbf{B}^*(\mathbf{q}) - \eta|\mathbf{k}|^2\mathbf{B}(\mathbf{k}), \quad (9)$$

$$\mathbf{k}\cdot\mathbf{u}(\mathbf{k}) = 0, \quad (10)$$

$$\mathbf{k}\cdot\mathbf{B}(\mathbf{k}) = 0, \quad (11)$$

where each sum denotes a double sum on all $\mathbf{p}$ and $\mathbf{q}$ forming a triad with $\mathbf{k}$ satisfying $\mathbf{k}+\mathbf{p}+\mathbf{q} = 0$, the dotted $\mathbf{u}$ and $\mathbf{B}$ denoting their time derivatives and the asterisk the complex conjugation. This from of equations implies invariance in exchanging $\mathbf{p}$ and $\mathbf{q}$.

The Fourier coefficients of the vorticity and current density fields take the following form

$$\boldsymbol{\omega}(\mathbf{k}) = i\mathbf{k}\times\mathbf{u}(\mathbf{k}), \qquad \mathbf{J}(\mathbf{k}) = i\mathbf{k}\times\mathbf{B}(\mathbf{k}). \quad (12)$$

B. Energies transfers

The kinetic and magnetic energies are defined by

$$E_K(\mathbf{r}) = \frac{1}{2}\mathbf{u}^2, \quad E_M(\mathbf{r}) = \frac{1}{2}\mathbf{B}^2. \quad (13)$$

Their Fourier coefficients take the following form

$$E_K(\mathbf{k}) = \frac{1}{2}\Re\{\mathbf{u}(\mathbf{k})\cdot\mathbf{u}^*(\mathbf{k})\}, \quad (14)$$

$$E_M(\mathbf{k}) = \frac{1}{2}\Re\{\mathbf{B}(\mathbf{k})\cdot\mathbf{B}^*(\mathbf{k})\}, \quad (15)$$

where $\Re$ denotes the real part. After (8) and (9) we find

$$\frac{\mathrm{d}}{\mathrm{d}t}E_K(\mathbf{k}) = \frac{1}{2}\Re\{\dot{\mathbf{u}}(\mathbf{k})\cdot\mathbf{u}(\mathbf{k})\} = \frac{1}{2}\sum_{\triangle\mathbf{kpq}}\Re\{(\mathbf{u}(\mathbf{p}),\boldsymbol{\omega}(\mathbf{q}),\mathbf{u}(\mathbf{k}))\} + \frac{1}{2}\sum_{\triangle\mathbf{kpq}}\Re\{(\mathbf{J}(\mathbf{p}),\mathbf{B}(\mathbf{q}),\mathbf{u}(\mathbf{k}))\} - \nu|\mathbf{k}|^2E_K(\mathbf{k}), \quad (16)$$

$$\frac{\mathrm{d}}{\mathrm{d}t}E_M(\mathbf{k}) = \frac{1}{2}\sum_{\triangle\mathbf{kpq}}\Re\{(\mathbf{u}(\mathbf{p}),\mathbf{B}(\mathbf{q}),\mathbf{J}(\mathbf{k}))\} - \eta|\mathbf{k}|^2E_M(\mathbf{k}), \quad (17)$$

where $(\cdot,\cdot,\cdot)$ denotes the vector triple product. As (16) and (17) must be invariant exchanging $\mathbf{p}$ and $\mathbf{q}$, they can be written as

$$\left(\frac{\mathrm{d}}{\mathrm{d}t} + 2\nu|\mathbf{k}|^2\right)E_K(\mathbf{k}) = \frac{1}{2}\sum_{\mathbf{k}=\mathbf{p}+\mathbf{q}} S_{E_K}(\mathbf{k}|\mathbf{p},\mathbf{q}) \quad (18)$$

$$\left(\frac{\mathrm{d}}{\mathrm{d}t} + 2\eta|\mathbf{k}|^2\right)E_M(\mathbf{k}) = \frac{1}{2}\sum_{\mathbf{k}=\mathbf{p}+\mathbf{q}} S_{E_M}(\mathbf{k}|\mathbf{p},\mathbf{q}) \quad (19)$$

where $S_{E_K}(\mathbf{k}|\mathbf{p},\mathbf{q})$ and $S_{E_M}(\mathbf{k}|\mathbf{p},\mathbf{q})$ are the kinetic and magnetic energy transfer rates from modes $\mathbf{p}$ and $\mathbf{q}$ to mode $\mathbf{k}$. They are respectively defined by

$$S_{E_K}(\mathbf{k}|\mathbf{p},\mathbf{q}) = S^u_{E_K}(\mathbf{k}|\mathbf{p},\mathbf{q}) + S^B_{E_K}(\mathbf{k}|\mathbf{p},\mathbf{q}) \quad (20)$$

with

$$S^u_{E_K}(\mathbf{k}|\mathbf{p},\mathbf{q}) = \Re\{(\mathbf{u}(\mathbf{p}),\boldsymbol{\omega}(\mathbf{q}),\mathbf{u}(\mathbf{k}))\} + \Re\{(\mathbf{u}(\mathbf{q}),\boldsymbol{\omega}(\mathbf{p}),\mathbf{u}(\mathbf{k}))\}, \quad (21)$$

$$S^B_{E_K}(\mathbf{k}|\mathbf{p},\mathbf{q}) = \Re\{(\mathbf{J}(\mathbf{p}),\mathbf{B}(\mathbf{q}),\mathbf{u}(\mathbf{k}))\} + \Re\{(\mathbf{J}(\mathbf{q}),\mathbf{B}(\mathbf{p}),\mathbf{u}(\mathbf{k}))\}, \quad (22)$$

and

$$S_{E_M}(\mathbf{k}|\mathbf{p},\mathbf{q}) = \Re\{(\mathbf{u}(\mathbf{p}),\mathbf{B}(\mathbf{q}),\mathbf{J}(\mathbf{k}))\} + \Re\{(\mathbf{u}(\mathbf{q}),\mathbf{B}(\mathbf{p}),\mathbf{J}(\mathbf{k}))\}. \quad (23)$$

The kinetic energy in mode $\mathbf{k}$ is transfered from or towards the other modes $\mathbf{p}$ and $\mathbf{q}$ via two types of non linear interactions $S^u_{E_K}(\mathbf{k}|\mathbf{p},\mathbf{q})$ and $S^B_{E_K}(\mathbf{k}|\mathbf{p},\mathbf{q})$. For $\mathbf{B}=0$ only $S^u_{E_K}(\mathbf{k}|\mathbf{p},\mathbf{q})$ remains. The magnetic energy in mode $\mathbf{k}$ is transfered from or towards the other modes $\mathbf{p}$ and $\mathbf{q}$ via the non linear interaction $S_{E_M}(\mathbf{k}|\mathbf{p},\mathbf{q})$.

C. Helicities transfers

The kinetic helicity H_K, the magnetic helicity H_M and the cross helicity H_C play important roles in MHD turbulence since they are conserved in a limit of zero viscosity and diffusivity (it is true for H_K at $\mathbf{B}=0$ only). In real space helicities are defined as

$$H_K(\mathbf{r}) = \frac{1}{2}\boldsymbol{\omega}\cdot\mathbf{u}, \quad (24)$$

$$H_M(\mathbf{r}) = \frac{1}{2}\mathbf{A}\cdot\mathbf{B}, \quad (25)$$

$$H_C(\mathbf{r}) = \mathbf{u}\cdot\mathbf{B}, \quad (26)$$

where $\mathbf{A}$ is the magnetic vector potential (under the Coulomb gauge $\nabla\cdot\mathbf{A}=0$) defined by $\mathbf{B}=\nabla\times\mathbf{A}$ and its Fourier coefficient takes the form

$$\mathbf{A}(\mathbf{k}) = \frac{1}{|\mathbf{k}|^2} i\mathbf{k}\times\mathbf{B}(\mathbf{k}). \quad (27)$$

Their Fourier coefficients take the following form

$$H_K(\mathbf{k}) = \frac{1}{2}\Re\{\mathbf{u}(\mathbf{k})\cdot\boldsymbol{\omega}^*(\mathbf{k})\} = \frac{1}{2}\Re\{i\mathbf{k},\mathbf{u}(\mathbf{k}),\mathbf{u}^*(\mathbf{k})\} \quad (28)$$

$$H_M(\mathbf{k}) = \frac{1}{2}\Re\{\mathbf{A}(\mathbf{k})\cdot\mathbf{B}^*(\mathbf{k})\} = \frac{1}{2|\mathbf{k}|^2}\Re\{i\mathbf{k},\mathbf{B}(\mathbf{k}),\mathbf{B}^*(\mathbf{k})\}, \quad (29)$$

$$H_C(\mathbf{k}) = \frac{1}{2}\Re\{\mathbf{u}(k)\cdot\mathbf{B}^*(\mathbf{k})\}. \quad (30)$$

Finally the time evolution of $H_K(\mathbf{k})$, $H_M(\mathbf{k})$ and $H_C(\mathbf{k})$ take the form

$$\left(\frac{\mathrm{d}}{\mathrm{d}t}+2\nu|\mathbf{k}|^2\right)H_K(\mathbf{k}) = \frac{1}{2}\sum_{\mathbf{k}=\mathbf{p}+\mathbf{q}} S_{H_K}(\mathbf{k}|\mathbf{p},\mathbf{q}), \quad (31)$$

$$\left(\frac{\mathrm{d}}{\mathrm{d}t}+2\eta|\mathbf{k}|^2\right)H_M(\mathbf{k}) = \frac{1}{2}\sum_{\mathbf{k}=\mathbf{p}+\mathbf{q}} S_{H_M}(\mathbf{k}|\mathbf{p},\mathbf{q}), \quad (32)$$

$$\left(\frac{\mathrm{d}}{\mathrm{d}t}+(\nu+\eta)|\mathbf{k}|^2\right)H_C(\mathbf{k}) = \frac{1}{2}\sum_{\mathbf{k}=\mathbf{p}+\mathbf{q}} S_{H_C}(\mathbf{k}|\mathbf{p},\mathbf{q}), \quad (33)$$

where kinetic helicity transfer rate $S_{H_K}(\mathbf{k}|\mathbf{p},\mathbf{q})$ and cross helicity transfer rate $S_{H_C}(\mathbf{k}|\mathbf{p},\mathbf{q})$ can be split in two parts

$$S_{H_K}(\mathbf{k}|\mathbf{p},\mathbf{q}) = S^u_{H_K}(\mathbf{k}|\mathbf{p},\mathbf{q}) + S^B_{H_K}(\mathbf{k}|\mathbf{p},\mathbf{q}), \quad (34)$$

$$S_{H_C}(\mathbf{k}|\mathbf{p},\mathbf{q}) = S^u_{H_C}(\mathbf{k}|\mathbf{p},\mathbf{q}) + S^B_{H_C}(\mathbf{k}|\mathbf{p},\mathbf{q}), \quad (35)$$

each part being defined as

$$S^u_{H_K}(\mathbf{k}|\mathbf{p},\mathbf{q}) = \Re\{(\mathbf{u}(\mathbf{p}),\boldsymbol{\omega}(\mathbf{q}),\boldsymbol{\omega}(\mathbf{k}))\} + \Re\{(\mathbf{u}(\mathbf{q}),\boldsymbol{\omega}(\mathbf{p}),\boldsymbol{\omega}(\mathbf{k}))\}, \quad (36)$$

$$S^B_{H_K}(\mathbf{k}|\mathbf{p},\mathbf{q}) = \Re\{(\mathbf{J}(\mathbf{p}),\mathbf{B}(\mathbf{q}),\boldsymbol{\omega}(\mathbf{k}))\} + \Re\{(\mathbf{J}(\mathbf{q}),\mathbf{B}(\mathbf{p}),\boldsymbol{\omega}(\mathbf{k}))\}, \quad (37)$$

$$S_{H_M}(\mathbf{k}|\mathbf{p},\mathbf{q}) = \Re\{(\mathbf{u}(\mathbf{p}),\mathbf{B}(\mathbf{q}),\mathbf{B}(\mathbf{k}))\} + \Re\{(\mathbf{u}(\mathbf{q}),\mathbf{B}(\mathbf{p}),\mathbf{B}(\mathbf{k}))\}, \quad (38)$$

$$S^u_{H_C}(\mathbf{k}|\mathbf{p},\mathbf{q}) = \Re\{(\mathbf{u}(\mathbf{p}),\boldsymbol{\omega}(\mathbf{q}),\mathbf{B}(\mathbf{k}))\} + \Re\{(\mathbf{u}(\mathbf{q}),\boldsymbol{\omega}(\mathbf{p}),\mathbf{B}(\mathbf{k}))\} + \Re\{(\mathbf{u}(\mathbf{p}),\mathbf{B}(\mathbf{q}),\boldsymbol{\omega}(\mathbf{k}))\} + \Re\{(\mathbf{u}(\mathbf{q}),\mathbf{B}(\mathbf{p}),\boldsymbol{\omega}(\mathbf{k}))\}, \quad (39)$$

$$S^B_{H_C}(\mathbf{k}|\mathbf{p},\mathbf{q}) = \Re\{(\mathbf{J}(\mathbf{p}),\mathbf{B}(\mathbf{q}),\mathbf{B}(\mathbf{k}))\} + \Re\{(\mathbf{J}(\mathbf{q}),\mathbf{B}(\mathbf{p}),\mathbf{B}(\mathbf{k}))\}. \quad (40)$$

Having definitions (21)-(23) and (36)-(40) one can introduce the mode-to-mode transfers and fluxes which define scale exchanges of velocity and magnetic fields by energy and helicities. Kinetic energy transfer can be expressed as

$$S^u_{E_K}(\mathbf{k}|\mathbf{p},\mathbf{q}) = T^u_{E_K}(\mathbf{k}|\mathbf{p}|\mathbf{q}) + T^u_{E_K}(\mathbf{k}|\mathbf{q}|\mathbf{p}), \quad (41)$$

where $T^u_{E_K}(\mathbf{k}|\mathbf{q}|\mathbf{p})$ is the kinetic energy transfer from mode $\mathbf{p}$ (the giver) to mode $\mathbf{k}$ (the receiver) via the mode $\mathbf{q}$ (the mediator). Then from Eq. (21) we can define

$$T^u_{E_K}(\mathbf{k}|\mathbf{p}|\mathbf{q}) = \Re\{(\mathbf{u}(\mathbf{q}),\boldsymbol{\omega}(\mathbf{p}),\mathbf{u}(\mathbf{k}))\}, \quad (42)$$

$$T^u_{E_K}(\mathbf{k}|\mathbf{q}|\mathbf{p}) = \Re\{(\mathbf{u}(\mathbf{p}),\boldsymbol{\omega}(\mathbf{q}),\mathbf{u}(\mathbf{k}))\}. \quad (43)$$

It satisfies necessary condition

$$T^u_{E_K}(\mathbf{k}|\mathbf{p}|\mathbf{q}) = -T^u_{E_K}(\mathbf{q}|\mathbf{p}|\mathbf{k}). \quad (44)$$

Systematic introduction of all expressions can be found in [5] (non-local transfers were implemented in shell models in [6]). Energy transfer among Fourier modes, energy flux, and shell-to-shell energy transfers are important quantities in MHD turbulence. They are in the basis of statistical theory of magnetohydrodynamic turbulence [7].

III. TARANG CODE

TARANG (synonym for waves in Sanskrit) is a general-purpose flow solver for turbulence and instability studies. It is a parallel and modular code written in object-oriented language C++, and it can solve incompressible flows involving pure fluid, Rayleigh-Bénard convection (RBC), passive and active scalars, magnetohydrodynamics (MHD), liquid-metals, rotating turbulence etc [4]. TARANG is an open-source code and it can be downloaded from *http://turbulencehub.org*.

Basic numerical structure of TARANG for all solvers follows pseudospectral method [8], [9]. The Navier-Stokes and related equations are numerically solved given an initial condition of the fields. The equations are time advanced using a time stepping method, e.g., the fourth-order Runge-Kutta scheme. The nonlinear terms, e.g. $\widehat{u_l u_j}$ and $\widehat{u_l B_j}$ become convolutions in spectral space whose computation requires $O(N^6)$

floating point operations for a N^3 grid. Orszag promoted the idea of using Fast Fourier Transform (FFT) with which a convolution is computed in $O(N^3 \log(N^3))$ operations [8]. For the computation of $\widehat{u_l u_j}$, $\widehat{u}_l(k)$ is transformed to real space $u_l(r)$, the product $u_l u_j$ is computed in the real space, and then the product is transformed back to the Fourier space. Since the computation of the nonlinear terms involves multiplication in real space, this method is called *pseudospectral method*. The procedure however suffers from *aliasing* errors, which is solved by filling up only 2/3 part of the array in each direction. See Boyd [9], Canuto *et al.* [8], Verma [4] for details.

The forward and inverse FFT operations take $\approx 80\%$ of the total time in a pseudospectral code. Therefore, one of the most efficient parallel FFT routines, FFTK (Fast Fourier transform Kanpur) [10] is used in TARANG. *A pencil decomposition* is implemented in FFTK and in the spectral code, which allows usage of maximum of N^2 cores for a N^3 grid simulations. Recently, Chatterjee *et al.* [10] scaled FFTK and TARANG up to grid resolution of 8192^3 grid using 65536 cores of Blue Gene/P and 196608 cores of Cray XC40 supercomputers (Shaheen I and II respectively of KAUST). This is the largest reported scaling of FFT in literature.

In Tarang, each step of the solution of Eqs. (1, 2) using variables $\mathbf{u}, \mathbf{B}$ requires 27 FFTs. However, the number of FFTs are reduced to 15 when Elsässer variables are used, thus saving computational time [4]. Also note that a MHD simulation requires 27 arrays for variables $\mathbf{u}(\mathbf{k}), \mathbf{B}(\mathbf{k}), \mathbf{u}(\mathbf{r}), \mathbf{B}(\mathbf{r}), \mathbf{F^u}(\mathbf{k}), \mathbf{F^B}(\mathbf{k}), \mathbf{nlin^u}(\mathbf{k}), \mathbf{nlin^B}(\mathbf{k})$, and three temporary arrays. Hence, a 1024^3 MHD simulations with double precision requires more than $27 \times 8 = 216$ Gigabytes of memory. For most simulations, $F^B(k) = 0$, but we have kept it in our design keeping in mind that TARANG is a general partial differential equation solver. Tarang employs explicit time-integration for the nonlinear term. The diffusive terms however solved using exponential trick [4].

Below we mention a few results that were obtained using the code. TARANG has been used for studying RBC in two (2D) and three (3D) dimensions [11]. Large resolution simulations of stably stratified flows and RBC [12] showed that stably stratified flows exhibit Bolgiano-Obukhov (BO) scaling in the buoyancy-dominated regime. Turbulent convection, however, exhibits Kolmogorov's spectrum rather than the BO spectrum. TARANG also used for performing simulations of MHD flows. Dynamo simulations [13] for the magnetic Prandtl number $\mathrm{Pm} = 20$ demonstrated that the magnetic energy growth is caused by nonlocal energy transfers from the large-scale or forcing-scale velocity field to small-scale magnetic field. Nonhelical MHD simulations [14] showed that the large-scale magnetic field can grow in nonhelical MHD when random external forcing is employed at scale 1/10 the box size. The energy fluxes and shell-to-shell transfer rates show that the large-scale magnetic energy grows due to the energy transfers from the velocity field at the forcing scales.

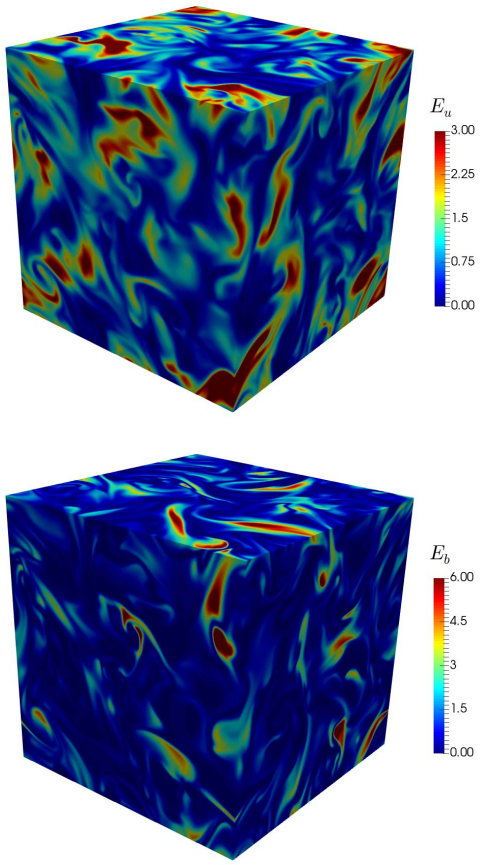

Fig. 1. Results for 512^3 grid simulation of MHD turbulence at $\nu = 0.008$, $\eta = 0.004$: distributions of kinetic (top) and magnetic (bottom) energies.

A. Forcing

The injection of energy, kinetic helicity and cross helicity into the flow is provided by the action given by the volumetric force $\mathbf{F}$. The properties of the force will influence the nature of the turbulence being realized. The specific choice of the parametrization plays an important role and determines the possibilities of a study. Special forcing constrains in MHD simulation with shell models allow to distinguish particular effects of magnetic helicity [15] and cross helicity [16]. To implement a turbulent cascade with an inertial interval, the force usually acts only in the range of large scales $k_0 \leq |\mathbf{k}| \leq k_1$, which is specified by two values of the wave numbers k_0 and k_1. Turbulent flow can be excited as a strictly deterministic force, i.e. which depends on velocity and magnetic fields or a force having a random component. Both options are implemented in the TARANG code. Here we show an example of a parametrization of deterministic forces that consists of three terms:

$$\mathbf{F} = \frac{\alpha \mathbf{u}}{|\mathbf{u}|^2} + \frac{\beta \boldsymbol{\omega}}{|\boldsymbol{\omega}||\mathbf{u}|} + \frac{\gamma \mathbf{b}}{|\mathbf{b}||\mathbf{u}|}, \tag{45}$$

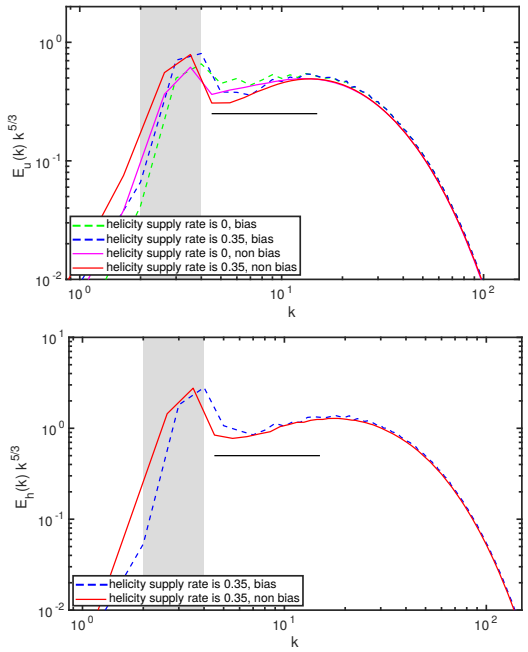

Fig. 2. Results for 512^3 grid, helical hydrodynamic turbulence, $\nu = 0.001$, energy supply rate is 0.1. Kinetic energy (top) and kinetic helicity (bottom) spectra are normalized by "$-5/3$" power law. The forcing is applied in the wave number band $2 \leq k \leq 4$, which is indicated in figure using a grey color.

where α, β and γ control injection rate of kinetic energy, kinetic helicity and cross helicity, respectively. As an example for $\alpha = 3$, $\beta = 1$ and $\gamma = 0$, Fig. 1 shows instant distributions of kinetic and magnetic energies at saturated nonlinear state of the small scale dynamo. One can see that structures of the magnetic field obeys the same turbulent scale as the kinetic energy.

B. Implementation of spectra calculation

The energy spectral density $E(k)$ is a well-known diagnostic of homogeneous turbulence and magnetohydrodynamic turbulence. However in most of the curves plotted by different authors, some systematic kinks can be observed at $k = 9$, $k = 15$ and $k = 19$. These kinks have no physical meaning, and are the artifacts of the method which is used to estimate $E(k)$ from a 3D grid. Instead of widely used formula

$$E_n = \sum_{n<|\mathbf{k}'|\leq n+1} \hat{E}(\mathbf{k}'), \tag{46}$$

another method can be implemented, in order to get rid of the spurious kinks and to estimate $E(k)$ much more accurately [17]. Main solution of the problem consists in an exact adjustment of the assumption that the number of points is proportional to the shell volume. All spectral densities in the TARANG code are calculated by

$$E_n = \frac{4\pi}{M_n} \sum_{n<|\mathbf{k}'|\leq n+1} \hat{E}(\mathbf{k}')|\mathbf{k}'|^2, \tag{47}$$

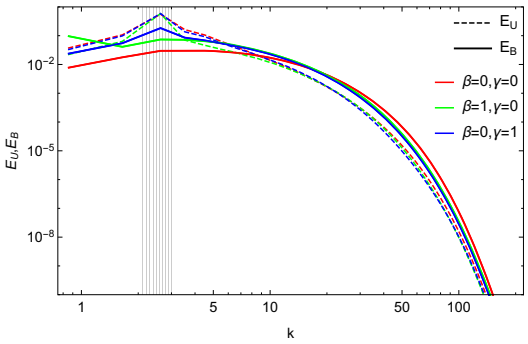

Fig. 3. Kinetic and magnetic energy spectra.

where again M_n is the number of vectors $\mathbf{k}'$ belonging to shell $n < |\mathbf{k}'| \leq n+1$ with an assigned wave number

$$k_n = \frac{1}{M_n} \sum_{n<|\mathbf{k}'|\leq n+1} |\mathbf{k}'|. \tag{48}$$

We perform the direct numerical simulation of the helical hydrodynamic turbulence with $\nu = 0.001$ for 512^3 grid to compare spectra calculated by (46) and (47) (see Fig. 2).

C. Implementation of fluxes calculation

We use the above formalism to compute various spectral transfer diagnostics. The energy flux $\Pi(k_0)$, defined as the energy emanating from the wave number sphere of radius k_0, is computed using the following formula:

$$\Pi^u_{E_K}(k_0) = \sum_{k>k_0} \sum_{p\leq k_0} T^u_{E_K}(\mathbf{k}|\mathbf{p}|\mathbf{q}). \tag{49}$$

It corresponds to running over all possible triad which is impossible to do in practice even for low resolution simulations. A trick to overcome this limitation is to make a convolution of the Fourier modes in the physical space. We use (21) to derive energy transfers from a set of Fourier modes in a region with $k \leq k_0$ (A) to another set of modes in region with $k > k_0$ (B):

$$\begin{aligned} \Pi^u_{E_K}(k_0) &= \Re\{\sum_{\mathbf{k}\in B}[\sum_{\mathbf{p}\in A} \mathbf{u}(\mathbf{q}) \times \boldsymbol{\omega}(\mathbf{p})^A \\ &+ \mathbf{u}(\mathbf{p}) \times \boldsymbol{\omega}(\mathbf{q})^A] \cdot \left[\mathbf{u}^B(\mathbf{k})\right]\} \\ &= \Re\{\sum_{\mathbf{k}\in B} [\mathbf{N}(\mathbf{k})] \cdot \left[\mathbf{u}^B(\mathbf{k})\right]\}, \end{aligned} \tag{50}$$

where

$$\mathbf{u}^{A,B}(\mathbf{k}) = \begin{cases} \mathbf{u}(\mathbf{k}) & \text{for } \mathbf{k} \in (A,B) \\ 0 & \text{otherwise} \end{cases} \tag{51}$$

and nonlinear $\mathbf{N}(\mathbf{k})$ is calculated in the physical space but the sum of $[\mathbf{N}(\mathbf{k})] \cdot [\mathbf{u}^B(\mathbf{k})]$ is taken in the Fourier space. We have implemented the all transfer functions in the TARANG code. Additional computational expenses coursed by direct and Fourier transforms are much less costly than the direct integration by definition (49).

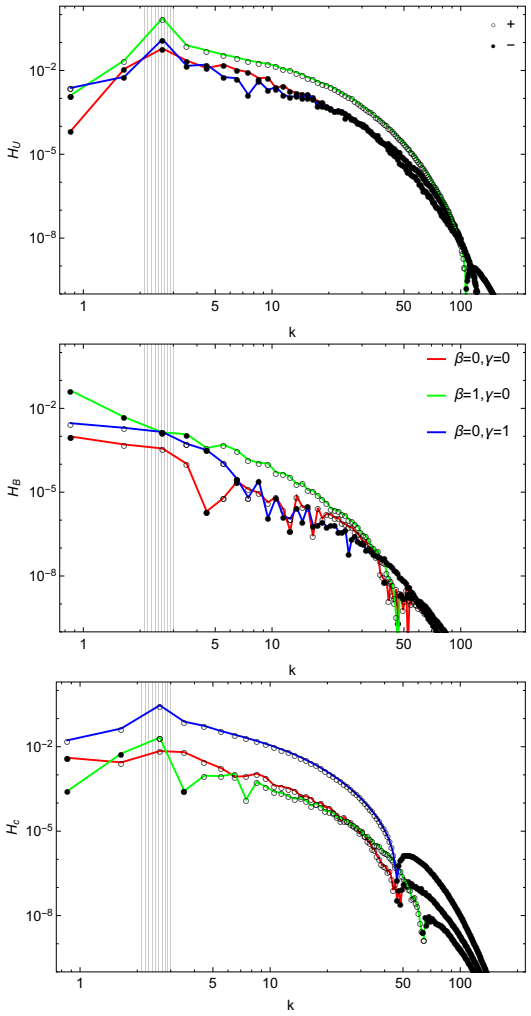

Fig. 4. Kinetic, magnetic and cross helicity spectra. Positive and negative values of helicity are denoted by open and close circles, correspondingly.

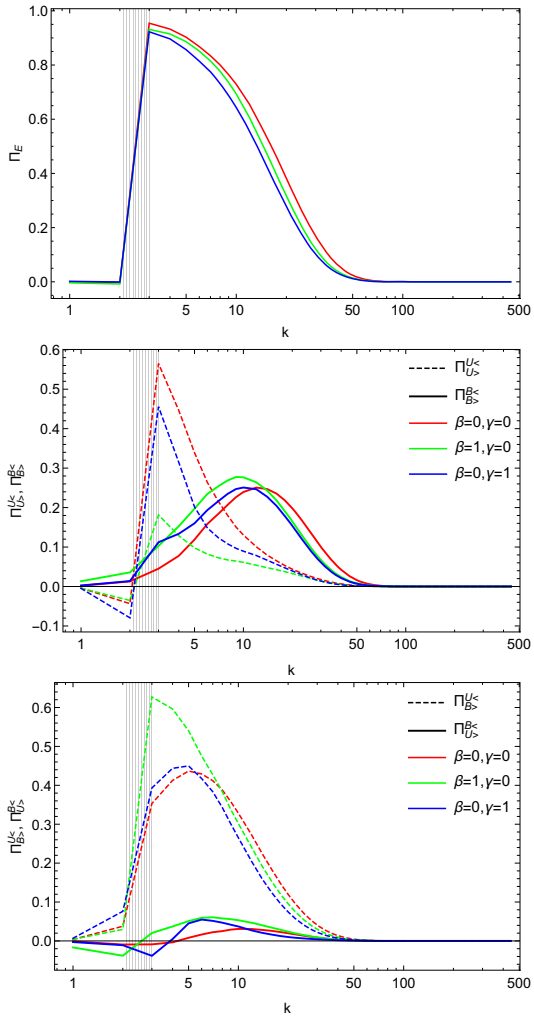

Fig. 5. Total energy flux and its components.

IV. Simulations of MHD turbulence with kinetic and cross helicity injection

We show spectra of kinetic and magnetic energies (see Fig. 3), helicity spectra (see Fig. 4), energy fluxes (see Fig. 5) and helicity fluxes (see Fig. 6 and Fig. 7) for DNS in 512^3 with $\nu = 0.008$ and $\eta = 0.004$. α is always adjusted to provide a unit injection rate of helicity. Three cases of forcing parameters are considered which correspond to: no helicity injection ($\beta = 0$, $\gamma = 0$), kinetic helicity injection ($\beta = 1$, $\gamma = 0$) and cross helicity injection ($\beta = 0$, $\gamma = 1$).

In the case of the kinetic helicity forcing we find a generation of magnetic field at largest scale. It corresponds to so-called nonlinear alpha-effect related to the inverse cascade [18]. However the total energy flux Π_E is zero in range of scales $1 \leq k \leq 2$. We can observe a dual cascade in its components only: $\Pi_{U>}^{U<}$ and $\Pi_{U>}^{B<}$ are negative (inverse) and $\Pi_{B>}^{B<}$ and $\Pi_{B>}^{U<}$ are positive (direct). Direct cascade from forcing scales to the small scales by $\Pi_{U>}^{U<}$ is significantly reduced due to effect of kinetic helicity (see various scenarios of helical turbulence in [19]–[21]). We note that the total magnetic helicity is conserved at zero value but it appears at large and small scales with an opposite sign.

In the case of the cross helicity forcing we find a peak of magnetic field at the forcing scale. It means that such flow is more efficient in the sense of local magnetic field generation. One see a particular changes of kinetic helicity fluxes as a result of cross helicity cascade [16].

V. Conclusions

We have described the possibilities of direct numerical simulation and postprocess analysis of MHD turbulence using the TARANG code. We have focused on the built-in postprocessing functions for analysis of spectral distributions and spectral energy and helicity transfers in homogeneous and isotropic MHD turbulence forced in a cubic region with

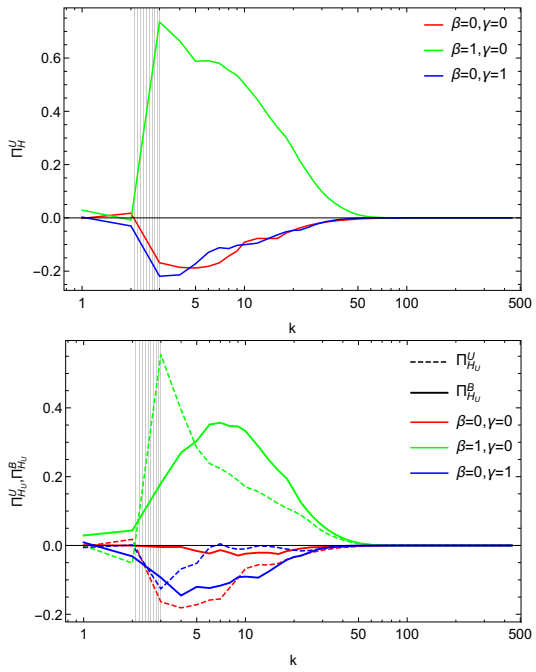

Fig. 6. Total kinetic helicity flux and its components.

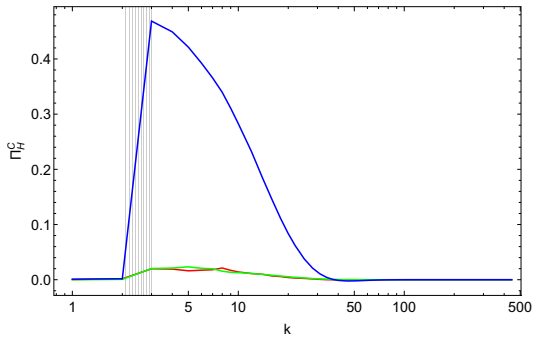

Fig. 7. Cross helicity flux.

periodic boundaries. Self-consistent mathematical description and numerical realization of spectra transfers are suggested. It gives a comprehensive inside view in the nonlinear process of the small scale dynamo.

ACKNOWLEDGMENT

This work was supported by joint project of the Russian Science Foundation (grant RSF-16-41-02012) and the Department of Science Technology of the Ministry of Science and Technology of the Republic of India (grant INT/RUS/RSF/3). Our numerical simulations were performed at Cray XC40 Shaheen II at KAUST supercomputing laboratory (KSL), Saudi Arabia through project K1052.

REFERENCES

[1] K.-H. Rädler, "Mean-field dynamo theory: early ideas and today's problems," in *Magnetohydrodynamics: Evolution of Ideas and Trends*, R. M. S. Molokov and H. K. Moffatt, Eds. Springer, 2007, pp. 55–72.
[2] A. Brandenburg, D. Sokoloff, and K. Subramanian, "Current Status of Turbulent Dynamo Theory. From Large-Scale to Small-Scale Dynamos," *Space. Sci. Rev.*, vol. 169, pp. 123–157, Sep. 2012.
[3] D. D. Sokoloff, R. A. Stepanov, and P. G. Frick, "Dynamos: from an astrophysical model to laboratory experiments," *Physics Uspekhi*, vol. 57, pp. 292–311, Mar. 2014.
[4] M. K. Verma, A. G. Chatterjee, R. K. Yadav, S. Paul, M. Chandra, and R. Samtaney, "Benchmarking and scaling studies of pseudospectral code Tarang for turbulence simulations," *Pramana-J. Phys.*, vol. 81, no. 4, pp. 617–629, Sep. 2013.
[5] F. Plunian, R. Stepanov, and P. Frick, "Shell models of magnetohydrodynamic turbulence," *Physics Reports*, vol. 523, pp. 1–60, Feb. 2013.
[6] F. Plunian and R. Stepanov, "A non-local shell model of hydrodynamic and magnetohydrodynamic turbulence," *New Journal of Physics*, vol. 9, p. 294, Aug. 2007.
[7] M. K. Verma, "Statistical theory of magnetohydrodynamic turbulence: recent results," *Phys. Rep.*, vol. 401, pp. 229–380, Nov. 2004.
[8] C. Canuto, M. Y. Hussaini, A. Quarteroni, and T. A. Zhang, *Spectral Methods in Fluid Turbulence*. Berlin: Springer, 1988.
[9] J. P. Boyd, *Chebyshev and Fourier Spectral Methods*, 2nd ed. Dover, 2013.
[10] A. G. Chatterjee, M. K. Verma, A. Kumar, R. Samtaney, B. Hadri, and R. Khurram, "Scaling of a fast fourier transform and a pseudo-spectral fluid solver up to 196608 cores," *J. Parallel Dist. Comput.*, no. https://doi.org/10.1016/j.jpdc.2017.10.014, 2017.
[11] A. Pandey, M. K. Verma, A. G. Chatterjee, and B. Dutta, "Similarities between 2D and 3D convection for large Prandtl number," *Pramana-J. Phys.*, vol. 87, no. 1, p. 13, Jun. 2016.
[12] A. Kumar, A. G. Chatterjee, and M. K. Verma, "Energy spectrum of buoyancy-driven turbulence," *Phys. Rev. E*, vol. 90, no. 2, p. 023016, Aug. 2014.
[13] R. Kumar, M. K. Verma, and R. Samtaney, "Energy transfers and magnetic energy growth in small-scale dynamo," *EPL*, vol. 104, no. 5, p. 54001, Jan. 2014.
[14] R. Kumar and M. K. Verma, "Amplification of large-scale magnetic field in nonhelical magnetohydrodynamics," *Physics of Plasmas*, vol. 24, no. 9, p. 092301, Sep. 2017.
[15] R. Stepanov, P. Frick, and I. Mizeva, "Joint Inverse Cascade of Magnetic Energy and Magnetic Helicity in MHD Turbulence," *Astrophys. J. Lett.*, vol. 798, p. L35, Jan. 2015.
[16] I. A. Mizeva, R. A. Stepanov, and P. G. Frik, "The cross-helicity effect on cascade processes in MHD turbulence," *Physics - Doklady*, vol. 54, pp. 93–97, Feb. 2009.
[17] R. Stepanov, F. Plunian, M. Kessar, and G. Balarac, "Systematic bias in the calculation of spectral density from a three-dimensional spatial grid," *Phys. Rev. E*, vol. 90, no. 5, p. 053309, Nov. 2014.
[18] A. Brandenburg, "The Inverse Cascade and Nonlinear Alpha-Effect in Simulations of Isotropic Helical Hydromagnetic Turbulence," *Astrophys. J.*, vol. 550, pp. 824–840, Apr. 2001.
[19] T. Lessinnes, F. Plunian, R. Stepanov, and D. Carati, "Dissipation scales of kinetic helicities in turbulence," *Physics of Fluids*, vol. 23, no. 3, pp. 035 108–035 108, Mar. 2011.
[20] R. A. Stepanov, P. G. Frik, and A. V. Shestakov, "Spectral properties of helical turbulence," *Fluid Dynamics*, vol. 44, pp. 658–666, Nov. 2009.
[21] R. Stepanov, E. Golbraikh, P. Frick, and A. Shestakov, "Hindered Energy Cascade in Highly Helical Isotropic Turbulence," *Physical Review Letters*, vol. 115, no. 23, p. 234501, Dec. 2015.